Energy and Thermofluids Engineering

Available at https://asps-journals.com

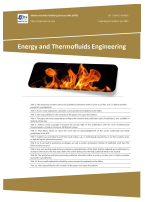

Numerical Analysis of Fuels Type Effect on Combustion and Emissions of Turbo-Charged Direct Injection Engine

Hamza Bousbaa[1]✉, Zouaoui Benayad[2], Khatir Naima[3]

1 *National Polytechnic school MAURICE AUDIN, Mechanic Department, LTE Laboratory, BP 1523 El Mnaouer 31000- Oran, Algeria*

2 *Materials and reactive systems laboratory. Djillali Liabes university of Sidi bel Abbes, Algeria*

3 *University Center NAAMA, Mechanic Department, LTE Laboratory, BP 1523 El Mnaouer 31000- Oran, Algeria*

Received November 9, 2022

Revised February 2, 2023

Accepted February 2, 2023

Published online: February 13, 2023

Keywords

CONVERGE Code

Diesel engine

Polluting gases

Fuels

Combustion

Abstract: One of the most important sources of contaminant emissions, especially in urban areas, is the car. Certain types of fuels are considered very beneficial in reducing emissions. The objective of this work is to study the effects of different types of fuels on the combustion and flow characteristics through the modeling of a direct injection turbocharged diesel engine. In this study, the simulation of combustion and pollutant emission evolution of an engine alimented with five fuels ($C_{14}H_{30}$, $C_{16}H_{34}$, C_8H_{18}, C_5H_{12}, and C_2H_5OH) was performed with CONVERGE CFD software. The results obtained confirm that the diesel engine is more powerful than an engine powered by light fuels such as gasoline. Injection of $C_{16}H_{34}$ and $C_{14}H_{30}$ resulted in higher pressure, temperature, and heat rate than C_8H_{18} (15.17% and 12.8% for pressure, 25.12% and 24.4% for temperature, and 54.54% and 31.81% for heat rate compared to C_8H_{18}). For polluting gases, if the engine is powered by heavy fuel oil, there are fewer unburned hydrocarbons and carbon monoxide, on the other hand, more soot and NOx, compared to C_8H_{18}. For the gaseous pollutants, the injection of the $C_{14}H_{30}$ generates more NOx and soot but less HC and CO (58.3%, 49.23%, 51.61%, and 2% respectively compared to C_8H_{18}). On the other hand, injection of C_2H_5OH generates a lower NOx and soot emissions level if compared to diesel (reduced levels by 75% and 95% respectively compared to diesel).

1. Introduction

The majority of internal combustion (IC) engines run on petroleum fuels, which are finite and will be depleted in around 35 years (Saurabh Kumar, 2017). Due to limited energy supplies, there is a risk of future energy shortages. IC engines with less than 185 kW utilize over 1/3 of all petroleum fuels, and one of the important sources of pollution in the environment is the exhaust fume released by these engines.

Many pieces of research including Heywood, 1988; Pranab Das, 2015; Bousbaa, 2021, have been conducted in recent years on IC engines, to reduce exhaust emissions by altering operational factors such as injection parameters, fuel type, EGR, and AdBlue.

As a result, many technologies have been used to reduce pollutant emissions in diesel engines, such as injection timing, injection pressure, and multiple injections (Okude et al. 2007), retarded injection timing (S. Gnanasekaran et al. 2016), HCCI mode operation (Miyamoto et al. 1999), EGR (P. Das et al. 2015), and high swirl ratio. Because of better spray atomization and air-fuel mixing, the Common Rail (CR) fuel injection system has a very high injection pressure, which can minimize particle emissions (Flaig et

✉ Corresponding author. E-mail address: hamza.bousbaa@enp-oran.dz

al. 1999). Experimenting with an engine by changing numerous settings is time-consuming due to the intricacy of practical implementation.

To better understand the complex phenomenon of combustion, currently, to study the parameters that influence the performance and evolution of pollutant emissions in automotive engines, numerical simulation has become one of the most powerful tools. Computational Fluid Dynamics (CFD) software CONVERGE, KIVA, STAR-CD, and others can be found in the market. They are used for the modeling and simulation of integrated circuit motors. It is possible to determine the temporal behavior of any variable of interest at any point in the computational domain by using numerical simulations. This results in a better and more in-depth understanding of the relevant processes necessary for their improvement.

In addition, the numerical simulation may be used to explore phenomena that occur over long time-scales or in inaccessible locations that cannot be investigated using traditional experimental methods. Sayin and Canakci (2009) investigated the effect of varying injection times in a diesel engine. When injection time was advanced, they discovered that NO_X and CO_2 emissions rose but unburned HC and CO emissions decreased. Multiple injections and split injection situations were analyzed quantitatively by Han et al (1996). They discovered that split injection greatly decreases soot without affecting NO_X emissions, and numerous injections significantly reduce NO_X emissions. Prasad et al. (2011) used extensive 3D CFD simulations to investigate the influence of varied piston bowl designs and injection timings on the combustion parameters of a CI engine. They discovered that at SOI of 8.60 BTDC, a strongly re-entrant piston bowl without a central projection was the optimum for swirl and intensification of TKE near TDC.

Jayashankara et al. (2010) used commercial CFD code to conduct numerical research on diesel engine simulation with respect to injection time and air boost pressure. They compared the flow-field findings from CFD modeling to the work by Payri et al. (2004) and found that advancing the injection timing resulted in an increase in cylinder pressure, cylinder temperature, and NOx emissions. Simulation of supercharged and intercooled engines resulted in increased NOx emissions when compared to normally aspirated engines. Yu et al. (2017) studied methanol, ethanol, and butanol-gasoline blends' effect under various alcohol ratios on combustion, performance, and emissions of engine characteristics. They concluded that due to the oxygen in ethanol and butanol-gasoline blends which improves combustion quality, HC emissions decreased, while they were increased with the other fuels. However, alcohols-gasoline blends presented lower NOx emissions and BTE decrease. For the butanol-gasoline blends, the results indicate showed a lower BSFC for its higher LHV.

Algayyim et al. (2018) studied the effect of injector hole diameter on the evolution spray behavior of butanol-diesel blends. In their conclusion, through the injection parameters, they can control the engine performance efficiency. Salman et al. (2019) used GT-Power Model to study the effect of injection timing on performance and pollutants emission in turbocharged diesel engines fuelled with Butanol-Diesel blends (5%, 15%, and 25% by volume). The results showed a lower amount of NOx and CO pollutants with the addition of butanol to diesel fuel, on the contrary, the HC and CO2 emissions are elevated. For the advance of the injection, a slight improvement is noticed in the thermal efficiency. On the other hand, the delay in the time of injection showed good results concerning the BTE. In addition, on the snapshot a rate of heat release and minimal pollution of HC, CO, and NOx. Samet et al. (2019) published an experimental study to improve performance and emissions in a spark ignition engine. They used Isoamyl alcohol/gasoline blends (30%, 20%, 10%, and 0%) at full load. Different CR (8.0:1, 8.5:1, and 9.0:1) and different values of speed (2600, 2800, 3000, and 3200 rpm) are used. The results show that the exhaust emissions decreased with isoamyl alcohol compared to gasoline at all CRs. In addition, the brake thermal efficiency increased by about 2.67% with a blend of 20% compared to gasoline on CR=9.0:1. The torque and effective power increased respectively by 2.03% and 2.51% with a blend of 20%. Zhiqing et al. (2022) used an AVL-Fire CFD code to study the effect of diesel/ethanol/n-butanol blends on combustion parameters, such as temperature, cylinder pressure, and pollutant emissions, such as NOx, CO, and soot. The results showed that diesel/ethanol/n-butanol blends reduced pressure and temperature, NOx, CO, and soot.

Hence, the present work aims to present a numerical simulation of combustion and emissions polluting (soot, NOX, HC, CO) in a direct injection engine fuelled by different fuels, utilizing code CONVERGE CFD (Richards et al. 2013). This research allows us to compare the combustion evolution and pollutants produced by various fuels in a quantifiable manner.

2. In-cylinder numerical investigation

2.1. Governing equations

In this part, we are using the CFD code CONVERGE (Richards et al. 2013) to perform a numerical investigation. In our numerical study, we worked on compression, atomization, spraying, combustion, and expansion.

The following governing differential equations are solved by the CFD code.

Continuity equations for species *m*:

$$\frac{\partial \rho_m}{\partial t}+\frac{\partial u_j \rho_m}{\partial x_j}=\frac{\partial}{\partial x_j}\left(\rho D \frac{\partial Y_m}{\partial x_j}\right)+S_m \quad (1)$$

Where; ρ is the total mass density, ρ_m is the mass density of species m, u is the velocity, D is the mass diffusion coefficient, Y_m is the mass fraction of species m, and S_m is the source term due to the chemistry and the spray.

With summation of the previous equation over all species, the total mass conservation equation becomes;

$$\frac{\partial \rho}{\partial t}+\frac{\partial \rho u_i}{\partial x_i}=S \quad (2)$$

Keeping mass constant in chemical reactions, the fluid momentum equation for the fluid mixture becomes:

$$\frac{\partial \rho u_i}{\partial t}+\frac{\partial \rho u_i u_j}{\partial x_j}=-\frac{\partial P}{\partial x_i}+\frac{\partial \sigma_{ij}}{\partial x_j}+S_i \quad (3)$$

where P is the fluid pressure, σ_{ij} is the stress tensor and S_i is the source term.

Finally, the internal energy equation becomes:

$$\frac{\partial \rho e}{\partial t}+\frac{\partial u_j \rho e}{\partial x_j}=-P\frac{\partial u_j}{\partial x_j}+\sigma_{ij}\frac{\partial u_i}{\partial x_j}+\frac{\partial}{\partial x_j}\left(K\frac{\partial T}{\partial x_j}\right)+\frac{\partial}{\partial x_j}\left(\rho D\sum_m h_m \frac{\partial Y_m}{\partial x_j}\right)+S \quad (4)$$

where e is the specific internal energy, K is the conductivity, h_m is the species enthalpy, and T is temperature.

2.2. Engine geometry and computational details

CONVERGE is used to simulate a one-cylinder DI diesel engine using the specs listed in Table 1. A periodic engine sector example is adapted for the engine simulation to save computing time. CONVERGE multiplies relevant physical variables in the output files by a suitable factor in the event of a periodic engine sector. Figure 1 shows the numerical mesh that was used to approximate 1/6 of the engine combustion chamber. The Converge pre-processor was used to make it. The use of symmetry lowered calculation time and memory requirements dramatically.

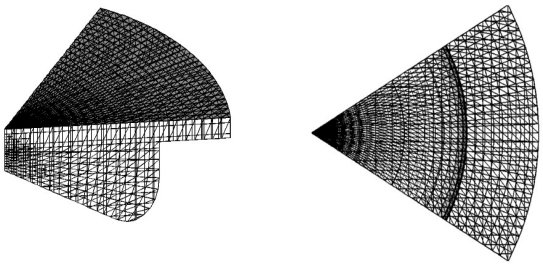

Fig. 1. Computational domain of the engine CATERPILLAR 3401

Table 1. Caterpillar 3401 Engine standard specification

Type	CATERPILLAR 3401
Bore	13.716 cm
Stroke	16.51 cm
Connecting rod length	26.3 cm
Engine Speed	1600 rpm
Squish	0.4221 cm
Compression ratio	15.1:1
No Nozzles	6
Duration of Injection	21°
Start of injection	9 c.a. degree BTDC

For the initial conditions, the temperature of the piston, cylinder head, and cylinder wall are based on experimental data. Note that the mesh is a dynamic mesh making the piston a mobile wall (see Table 2). The injection fuels and their specifications are shown in Table 3 with the important specifications of injection.

Table 2. Initial conditions

Initial fuel Temperature	344 K
Cylinder Wall Temperature	433 K
Piston Wall Temperature	553 K
Head Temperature	523

Table 3. Fuel injection system

Fuel injection system	
Fuels	$C_{14}H_{30}$, $C_{16}H_{34}$, C_8H_{18}, C_5H_{12}, C_2H_5OH
Injection mode	Profile
Injection system	Common Rail
Diameter of injection hole	$2{,}6*10e^{-4}$
Mass of fuel injected	0.1621 g/cycle

2.3. Computational Sub-models

CONVERGE is used for in-cylinder flow simulations, performance estimation, and combustion analysis in engines. It is a ground-breaking CFD software that overcomes the simulations generation bottleneck mesh.

The software solves Navier–Stokes equations using the approach of Finite Volume (Richards et al., 2013).

- **Spay model:**

A modified KH-RT model is utilized to predict the spray breakup, with the assumption that aerodynamic instabilities (KH) are responsible for the primary breakdown of the injected liquid blobs. Examining the competing effects of the RT processes is used to model the subsequent breakup of these dips. The KH-RT model has been proven to be faster and more accurate than the other CONVERGE models, such as O'Rourke's model (Richards et al., 2013).

- **Ignition and Combustion Models:**

A multistep kinetics model based on the Shell model (Richard et al., 2008) has been implemented in CONVERGE to model diesel ignition delay. The Shell model was developed to predict knocking in gasoline engines. To simulate auto-ignition in diesel engines, a simplified reaction mechanism was used. Eight reactions are given in this model by,

1. $C_nH_{2m} + O_2 \rightarrow 2R^*$
2. $R^* \rightarrow R^* + P + \text{Heat}$
3. $R^* \rightarrow R^* + B$
4. $R^* \rightarrow R^* + Q$
5. $R^* + Q \rightarrow R^* + B$
6. $B \rightarrow 2R^*$
7. $R^* \rightarrow \text{Termination}$
8. $2R^* \rightarrow \text{Termination}$

(5)

For the combustion simulation, the Time Combustion (CTC) model will be used. The variation of species density *m* is modeled as follows:

$$\frac{\partial \rho_m}{\partial t} = -\frac{\rho_m - \rho_m^*}{\tau_c} \tag{6}$$

Where ρ^* is the species density's local and instantaneous thermodynamic equilibrium value, and τ_c is the typical time to reach equilibrium. The characteristic time is computed using the following formula

$$\tau_c = \tau_{chem} + f\tau_{turb}, \tag{7}$$

where τ_{chem}, τ_{turb}, and f represent the chemical kinetics time, the turbulent mixing time, and the delay coefficient that replicates turbulence's increasing influence on combustion respectively. Further, the chemical time is given by the following expression (Richards et al., 2013):

$$\tau_{chem} = \frac{[C_nH_{2m}]^{0.75} e^{(E_{chem}/R_uT_g)}}{2A_{chem}[O_2]^{1.5}}, \tag{8}$$

where E_{chem}, A_{chem}, R_u, and T_g are the activation energy given, the constant set in the input files, the universal gas constant, and the gas temperature respectively. Further, the turbulent time is given by the following expression:

$$\tau_{turb} = C_2 \frac{k}{\varepsilon}, \tag{9}$$

C_2 is a constant in this equation. The turbulent timeframe functions as a sub-grid model for species non-uniformity in a cell. The combustion process may be slowed by the sub-grid non-uniformity of species, which cannot be properly accounted for. As a result, the turbulent timeframe is used to slow down the combustion process.

- Model for turbulence: (Richards et al., 2013)

The RNG k-ε model with fast distortion is engaged, and the normal k-constants are employed. This type is perfectly suited for this situation because it is built for quick compression or rapid expansion.

To properly model the temperatures near the wall or the resolution of a turbulent boundary layer is not sufficient; the law-of-the-wall must be used. In this study, the Han and Reitz (1997) model is used, this model accounts for compressible effects.

- Models of NO_X and Soot Formation: (Richards et al., 2013)

The expanded Zeldovich mechanism is used to describe the reaction process of NO_X production.

$$\begin{aligned} &N_2 + O \leftrightarrow NO + N \\ &N + O_2 \leftrightarrow NO + O \\ &N + OH \leftrightarrow NO + H \end{aligned} \tag{10}$$

Chemical species that exist in these global reactions are employed in the single-step fuel conversion equation as follows:

$$\frac{d[NO]}{dt} = 2k_f[N_2][O_2] \tag{11}$$

The Hiroyasu formation model was used to model soot emission in this investigation.

$$\frac{dm_s}{dt} = \frac{dm_{sf}}{dt} - \frac{dm_{so}}{dt} \tag{12}$$

where *m*, *sf,* and *so* denote the mass of soot, soot formed and soot oxidized respectively. For more information on this model, readers are referred to (Richards et al., 2013).

3. Results and discussions

The validation of the code is based on a comparison of experimental and numerical simulation results; the comparable quantity is the cylinder pressure for the 1600 rpm regime, which is shown in Figure 2. When compared to $C_{14}H_{30}$, it can be shown that the results are in good agreement with those obtained experimentally, with errors of less than 3%.

The SAGE model was used to forecast the combustion of light fuels C_8H_{18}, C_5H_{12}, and C_2H_5OH, while the CTC model was used to predict the combustion of heavy fuels $C_{14}H_{30}$ and $C_{16}H_{34}$. Figure 3 shows the greatest average pressure at TDC. Before TDC, the air is compressed to 70 bars, but during the combustion phase, it rises to 112 pressure, which gas oils attain after a short time at TDC, and 97 bars for gasoline after a short time at TDC, because of their properties such as calorific power, cetane, and octane number.

For the various fuels, Figure 4 predicts the average temperature evolution of the gases in the cylinder as a function of the crank angle. We see a quick temperature rise, indicating combustion. Because of the greater auto-

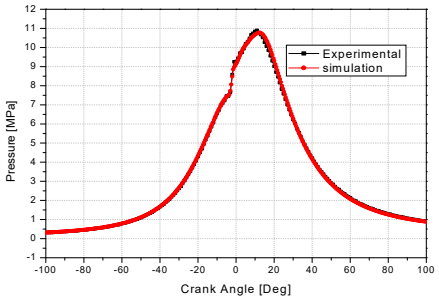

Fig. 2. Measured and Predicted in-Cylinder Pressure.

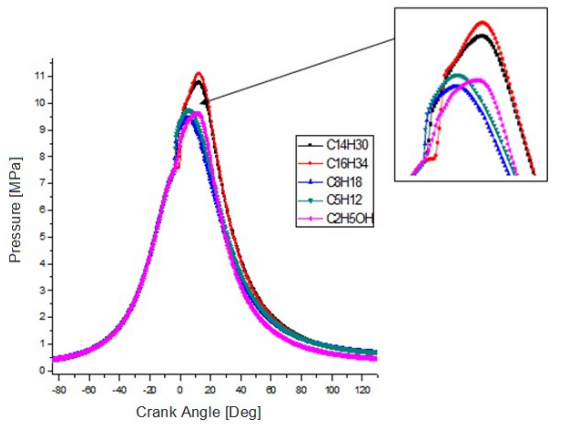

Fig. 3. Measured and Predicted in-Cylinder Pressure for different fuels.

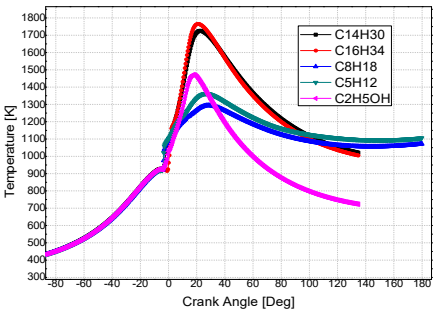

Fig. 4. Predicted temperatures for different fuels.

ignition delay (which results in a longer combustion period), the maximum average temperature for $C_{14}H_{30}$ and $C_{16}H_{34}$ is 1730K and 1800K, respectively, while the maximum average temperature for C_2H_5OH, C_8H_{18}, and C_5H_{12} is 1470K, 1325K, and 1390K, respectively. Figure 5 represents the development of the heat rate as a function of crank angle computed throughout an engine cycle for the five tested fuels. All of the tested fuels show a quick increase in heat rate, indicating burning. Because of the cetane number, the heat emitted by burning is more relevant in the case of $C_{14}H_{30}$ and $C_{16}H_{34}$ in contrast to the other tested fuels, according to the study of Figure 5 for gas oils. Furthermore, the $C_{16}H_{34}$ fuel has a longer auto-ignition delay owing to its low cetane number, but the light fuels C_8H_{18}, C_5H_{12}, and C_2H_5OH have a shorter auto-ignition delay due to their higher-octane rating (Heywood, 1988).

For the various fuels, Figure 6 depicts the Nitrogen Oxides development NO_X which is a function of the crankshaft angle. The combustion of C_2H_5OH emits less NO_X mass than others fuels, as can be shown. $C_{14}H_{30}$ and $C_{16}H_{34}$, on the other hand, produce a lot of NO_X when compared to C_5H_{12}

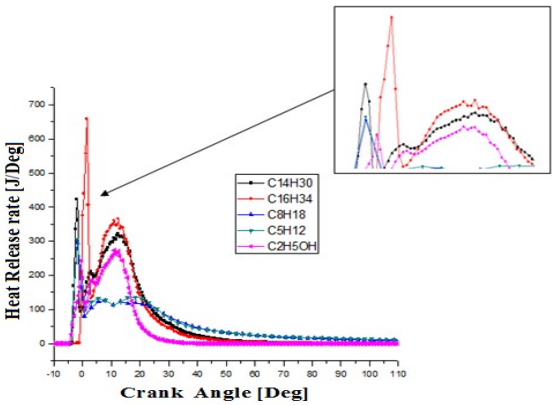

Fig. 5. Heat Release rate for different fuels.

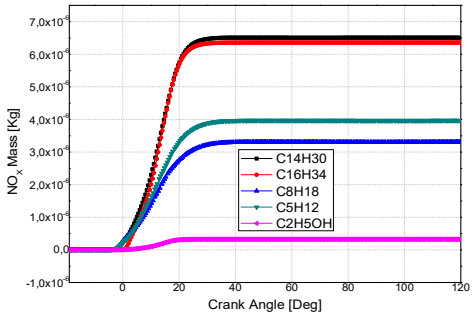

Fig. 6. Total mass of NO_X for different fuels

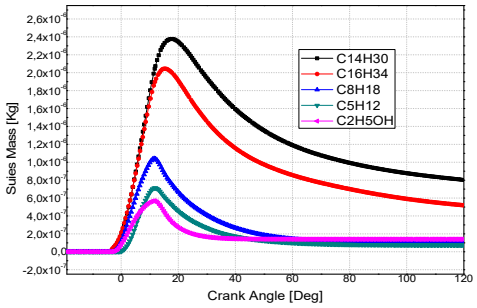

Fig. 7. Total mass of soot for different fuels.

and C_8H_{18}; their mass at the conclusion of the cycle is 6. 5× 10^{-5} g, 6.37×10^{-5}g, 4× 10^{-5}g and 3.4× 10^{-5}g, respectively. This results because of their properties such as density and viscosity which influences the quality of atomization and vaporization of spray.

For each fuel, Figure 7 depicts the development of soot as a function of crank angle. For light fuels, the amount of soot reaches a maximum value of around 10° after TDC and around 15° after TDC for heavy fuels and then falls towards the conclusion of the diffusion period. Due to the oxygen content that favors combustion, we found that soot emissions in the situation where the engine is fuelled with C_2H_5OH are much lower (approximately 5.5×10^{-7} g) than in the other studied scenarios.

The development of unburned hydrocarbons (HC) as a function of the crankshaft angle is seen in Figure 8. The combustion process is fully responsible for the hydrocarbon emissions. When compared to other fuels such as C_5H_{12} and C_8H_{18}, the combustion of $C_{14}H_{30}$ and $C_{16}H_{34}$ generates fewer unburned hydrocarbons. Despite having higher density and viscosity than other fuels, the rate of HC emission is lower when C_2H_5OH is used. This is likely owing to the oxygen component, which accelerates burning (Cheikh KEZRANE, 2016). Figure 9 depicts the development of CO as a function of the crankshaft angle for the investigated fuels. The mass fraction of CO remains practically constant during the self-ignition delay, and right before ignition, the reaction rate rises rapidly, resulting in a fast increase in the mass, which indicates combustion. At the end of the diffusion combustion phase, this mass tends to stabilize. After combustion, $C_{14}H_{30}$, $C_{16}H_{34}$, and C_2H_5OH have masses of roughly 0 g, whereas C_5H_{12} and C_8H_{18} have masses of 3×10^{-5}g and 5×10^{-5}g, respectively. For CO, between 10° and 15° after TDC, the quantity of gas increases until it reaches a maximum value, then falls as the combustion progresses. CO emissions are reduced when C_2H_5OH is burned. The same explanations as before may be used to explain this result: The hydrocarbons C_5H_{12}, C_8H_{18}, $C_{14}H_{30}$, and $C_{16}H_{34}$ lack local oxygen (Cheikh KEZRANE, 2016).

Figures 10 and 11 show the NOX and soot contours for just three fuels (at TDC and 40° after TDC). When compared to other fuels, we see that C14H30 emits a lot of NOX and soot. Furthermore, we discovered that when the engine is fuelled with C2H5OH, the NOX and soot concentrations are lower than when the engine is fueled with other fuels. The prior results (Figures 8 and 9) corroborated these findings.

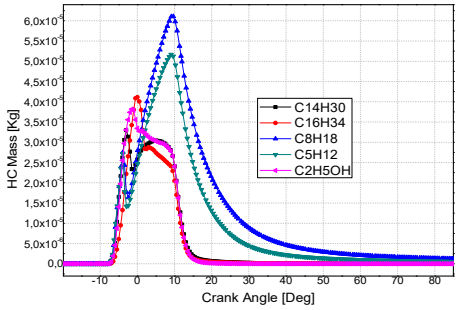

Fig. 8. Total mass of HC for different fuels.

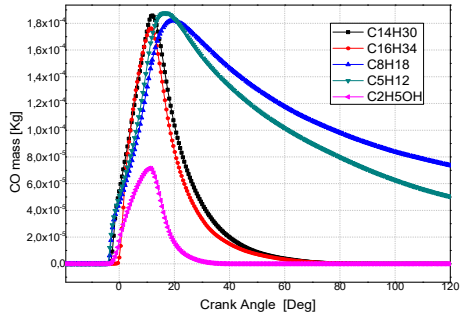

Fig. 9. Total mass of CO for different fuels.

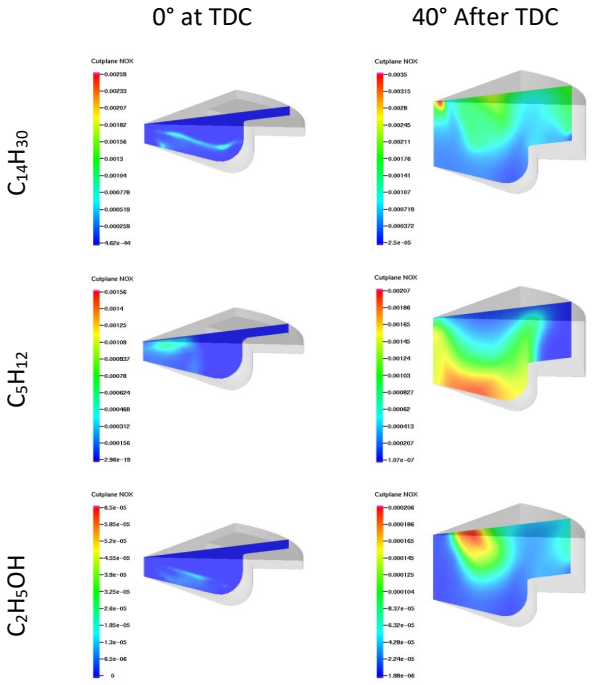

Fig. 10. NO_X mass contour for different fuels at different angles.

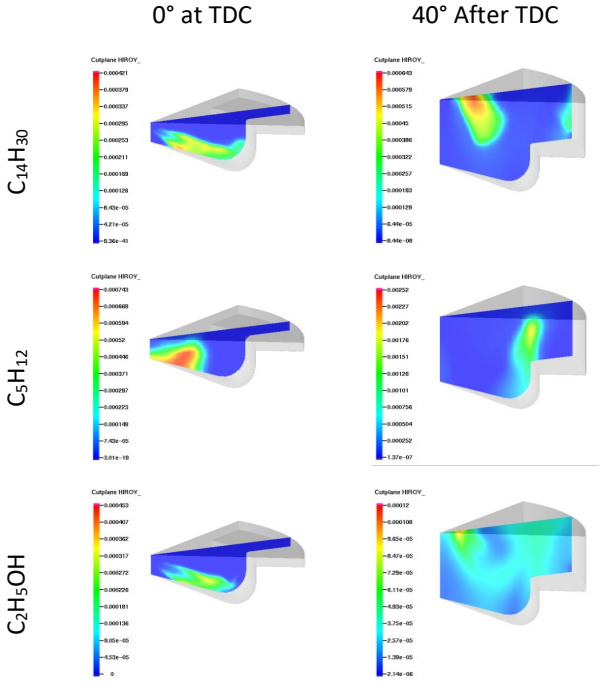

Fig. 11. Soot mass contour for different fuels at different angles.

CONCLUSION

To evaluate the effects of injection of five fuels on combustion and emissions pollution evolution. CONVERGE tool has been validated by the experimental data for in-cylinder pressure evolution. The main conclusions of this study are summarized as follows:

- $C_{16}H_{34}$ and $C_{14}H_{30}$ have higher pressure, temperature, and heat rate than C_8H_{18} (15.17% and 12.8% respectively for pressure, 25.12%, and 24.4% respectively for temperature, and 54.54% and 31.81% respectively for heat rate compared to C_8H_{18}).
- The diesel engine is more powerful than a motor powered by light fuels like gasoline.
- The heavy fuels (the most common being $C_{14}H_{30}$) generate more NO_X and soot but less HC and CO when it comes to gaseous pollutants (58.3%, 49.23%, 51.61%, and 2% respectively compared to C_8H_{18}).
- These findings suggest that the significant quantity of NO_X and soot created by gas oil combustion is an issue. It's the polar opposite for the species.
- C_2H_5OH can be considered an alternative fuel for engines (the reduced levels of NOX and soot emissions are 75% and 95%, respectively compared to diesel).
- This study adds to our understanding of the process of various fuels combusting in engines.

Disclosures

Free Access to this article is sponsored by SARL ALPHA CRISTO INDUSTRIAL.

Nomenclature

Greek symbols

σ	Viscous stress tensor
ε	Dissipation rate of turbulent kinetic energy
τ_c	Characteristic time scale of the chemical reaction
τ_t	Characteristic time scale of the turbulence
∇	Laplacian

Subscripts

ATDC	After Top Dead Center.
BTDC	Before Top Dead Center
BTE	Brake Thermal Efficiency
BSFC	Brake Specific Fuel Consumption
CA	Crank Angle
CR	Common Rail fuel injection system
CFD	Computational fluid dynamics
EGR	Exhaust Gas Recirculation
IC	Internal combustion
TDC	Top Dead Center
TKE	Turbulent Kinetic Energy
PMH	Point Mort High
SOI	Start of Injection
LHV	Lower Heating Value

References

Algayyim S, Wandel A, Yusaf T, The Impact of Injector Hole Diameter on Spray Behaviour for Butanol-Diesel Blends. Energies, 2018, 11(5),1298. https://doi.org/10.3390/en11051298.

Cenk Sayin, Mustafa Canakci (2009) Effects of injection timing on the engine performance and exhaust emissions of a dual-fuel diesel engine, Energy Conversion & Management, 50:203–13.

Cheikh KEZRANE, Abdelkader BENDRISS, Khaled LOUBAR, Awad SARY, Abdelkrim LIAZID, Mohand TAZEROUT (2016) COMPARAISON DES ÉMISSIONS POLLUANTES D'UN MOTEUR DIESEL ALIMENTÉ AVEC QUATRE CARBURANTS, ICEMAEP2016, October 30-31, Constantine,Algeria.

Flaig, U., W. Polach and G. Ziegler (1999) Common rail system (CR-system) for passenger car DI diesel engines; experiences with applications for series production projects. SAE Paper Nº 1999-01-0191.

Han Z, Uludogan A, Hampson GJ, Reitz, RD (1996) Mechanism of soot and NO_X emission reduction using multiple-injection in a diesel engine. SAE paper Nº 960633.

Han, Z. and Reitz, R. D., "A Temperature Wall Function Formulation for Variable Density Turbulence Flow with Application to Engine Convective Heat Transfer Modeling," Int. J. Heat and Mass Transfer, Vol. 40, 1997.

J.B. Heywood, (1988) Internal combustion engine fundamentals, Edition Mc Graw Hill.

Jayashankara B, Ganesan V (2010) Effect of fuel injection timing and intake pressure on the performance of a DI diesel engine – A parametric study using CFD, Energy Conversion and Management, 51: 1835–1848.

Lamia MEDJAHED, Hamza BOUSBAA (2021) Effect of injection parameters on combustion and emissions characheristics of a Turbocharged DI diesel engine-A CFD approach using CONVERGE, ICETS'21, May 22nd 24th, university Adrar, Algeria.

Miyamoto, T., A.K. Hayashi, A. Harada, S. Sasaki, A. Hisashi and K. Tujimura (1999) A computational investigation of premixed lean diesel combustion-characteristics of fuel-air mixture formation, combustion and emissions. SAE Paper Nº 1999-01-0229.

Okude, K., K. Mori, S. Shiino, K. Yamada and Y. Matsumoto, (2007) Effects of multiple injections on diesel emission and combustion characteristics. SAE Paper Nº. 2007-01-4178.

Pranab Das, P.M.V. Subbarao, J.P. Subrahmanyam (2015) Control of combustion process in an HCCI-DI combustion engine using dual injection strategy with EGR. JFUE 9414, 9 July 2015. Nº of Pages 10, Model 5G.

Prasad BVVSU, Sharma CS, Anand TNC, Ravikrishna RV (2011) High swirl-inducing piston bowls in small diesel engines for emission reduction. Applied Energy 88: 2355-67.

Payri F, Benajes J, Margot X, Gil A (2004) CFD modeling of the in-cylinder flow in direct injection diesel engines. Computers & Fluids, 33: 995–1021.

Richards, K. J., Senecal, P. K., and Pomraning, E (2013) CONVERGE (Version 2.1.0), Convergent Science, Inc., Middleton, WI.

Salman Abdu Ahmed, Song Zhou, Yuanqing Zhu, Yongming Feng, Adil Malik, Naseem Ahmad, Influence of Injection Timing on Performance and Exhaust Emission of CI Engine Fuelled with Butanol-Diesel Using a 1D GT-Power Model, Processes 2019, 7(5), 299; https://doi.org/10.3390/pr7050299.

Samet Uslu M, Bahattin Celik, Combustion and emission characteristics of isoamyl alcohol-gasoline blends in spark ignition engine, Fuel, 262, 2019, pp 1164-96.https://doi.org/10.1016/j.fuel.2019.116496.

Saurabh Kumar, March 27, 2017; Energy resources will be exhausted in 40 years: Expert, https://energy.economictimes.indiatimes.com/news/coal/energy-resources-will-be-exhausted-in-40-years-expert/57846890.

Sakthivel Gnanasekaran , Saravanan N., M. Ilangkumaran , (2016) Influence of injection timing on performance, emission and combustion characteristics of a DI diesel engine running on fish oil biodiesel. Energy 116 : 1218-1229.

Yu Li, Jinke Gong, Yuanwang Deng, Wenhua Yuan, Jun Fu, Bin Zhang, Experimental comparative study on combustion, performance and emissions characteristics of methanol, ethanol and butanol in a spark ignition engine, Applied Thermal Engineering, 115, 2017, pp 53-63. https://doi.org/10.1016/j.applthermaleng.2016.12.037.

Zhiqing Zhang, Jiangtao Li, Jie Tian, Rui Dong, Zhi Zou, Sheng Gao, Dongli Tan, Performance, combustion and emission characteristics investigations on a diesel engine fueled with diesel/ ethanol /n-butanol blends, Energy, 249 (15), 2022, 123733.